Available online at www.sciencedirect.com
ScienceDirect
Bioorganic & Medicinal Chemistry Letters 17 (2007) 4619–4624
Bioorganic & Medicinal Chemistry Letters

Design of novel histone deacetylase inhibitors

Phieng Siliphaivanh,[a,*] Paul Harrington,[a,†] David J. Witter,[a] Karin Otte,[a] Paul Tempest,[a] Sam Kattar,[a] Astrid M. Kral,[b] Judith C. Fleming,[b] Sujal V. Deshmukh,[a] Andreas Harsch,[a] Paul J. Secrist[b] and Thomas A. Miller[a]

[a]*Department of Drug Design & Optimization, Merck Research Laboratories, 33 Avenue Louis Pasteur, Boston, MA 02115, USA*
[b]*Department of Cancer and Biology Therapeutics, Merck Research Laboratories, 33 Avenue Louis Pasteur, Boston, MA 02115, USA*

Received 30 April 2007; revised 22 May 2007; accepted 24 May 2007
Available online 27 May 2007

Abstract—Histone deacetylase (HDAC) inhibitors that target Class I and Class II HDACs are of synthetic and therapeutic interest and ongoing clinical studies indicate that they show great promise for the treatment of cancer. Moreover, Zolinza[R] (vorinostat) was recently approved by the FDA for the treatment of the cutaneous manifestations of cutaneous T-cell lymphoma [*Nat. Rev. Drug Disc*. **2007**, *6*, 21]. As part of a broader effort to more fully explore the structure–activity relationships (SAR) of HDAC inhibitors, we sought to identify novel HDAC inhibitor structures through iterative design by utilizing low affinity ligands as synthetic starting points for SAR development. Novel and potent HDAC inhibitors have been identified using this approach and herein we report the optimization of the recognition elements of a novel series of malonyl-derived HDAC inhibitors.

HDAC inhibitors possess diverse biological activities and many of these agents have been demonstrated to be effective inhibitors of tumor growth in animal models of cancer.[1–5] With few exceptions, HDAC inhibitors can be broadly characterized by a common pharmacophore that summarizes key elements of inhibitor–enzyme interactions (Fig. 1).[1,3,6–10] Because most of the original HDAC inhibitors have been derived from relatively complex and potent natural products, a large number of efforts have focused on the refinement of the existing pharmacophore using designs that mimic those found in nature.[11–15] In contrast, few efforts have been undertaken to design HDAC inhibitors de novo using less complex, low-affinity synthetic starting points. Importantly, an inverse correlation between molecular complexity and lead tractability/quality has been noted in the literature.[16] This report details how less complex, lower affinity lead structures can represent unique starting points for SAR development. Moreover, this study demonstrates how iterative evolution of low-affinity leads can afford potent scaffolds with structures unique from those derived from traditional optimization of structurally complex, high-affinity lead structures culminating in a novel, potent HDAC inhibitor.

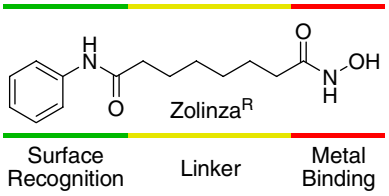

Figure 1. Summary of HDAC inhibitor structural characteristics.

As part of a broader effort to more fully explore the SAR of HDAC inhibitors, we have identified novel HDAC inhibitor structures through iterative design using acetohydroxamic acid **1** as a synthetic starting point for SAR development. We chose to use compound **1** because it represents a minimum structural requirement for HDAC inhibition through a well-defined interaction (IC_{50} = 625 μM). Namely, the hydroxamic acid moiety found in existing HDAC inhibitors has been shown to interact directly with the active-site zinc of the HDAC enzyme.[17] Having established the metal binding domain of the HDAC inhibitor pharmacophore (Fig. 1) as a hydroxamic acid for our initial efforts, we sought to iteratively optimize

Keywords: Histone deacetylases; Malonyl benzamides.
* Corresponding author. Tel.: +1 617 992 2055; fax: +1 617 992 2043; e-mail: Phieng_siliphaivanh@merck.com
† Present address: Department of Medicinal Chemistry, Amgen Inc., One Amgen Center Drive, Thousand Oaks, CA 91320-1799, USA.

0960-894X/$ - see front matter © 2007 Elsevier Ltd. All rights reserved.
doi:10.1016/j.bmcl.2007.05.080

the linker and surface recognition domains to obtain novel and potent HDAC inhibitors. The first round of optimization included the incorporation of alkyl, cyclic, and aromatic linker domain followed by recognition domains' incorporation and optimization. These studies revealed that hydrophobic aryl moieties are preferred over acyclic alkyl linker groups (Fig. 2). Thus, a potency increase of ~30-fold was observed for benzoyl hydroxamic acid **2** over alkyl-hydroxamates such as acetohydroxamic acid **1**.

Further modifications of the surface recognition domain by substitution on the aryl linker with *tert*-butyl (**3**) and then diphenylmalonamide (**4**) further enhanced activity to nanomolar levels (Fig. 2).

Having established **4** as a viable and potent lead structure, we sought to explore the application of this core scaffold with other potential zinc binding domains since hydroxamates are known to have short half-lives and generally poor pharmacokinetic properties. HDAC inhibitors containing an *N*-(2-aminophenyl) moiety in the metal binding domain are of significant clinical importance. [4,5,18,19] As such, to further explore the SAR of the malonyl-derived HDAC inhibitor **4**, the corresponding 2-aminophenyl benzamide analogue **5a**[20] became the focus of our synthetic efforts.

The synthesis of 2-aminophenyl benzamide analogues of **4** is shown in Scheme 1. *tert*-Butyl ester **6** was obtained by esterification of benzoyl chloride **7** with potassium

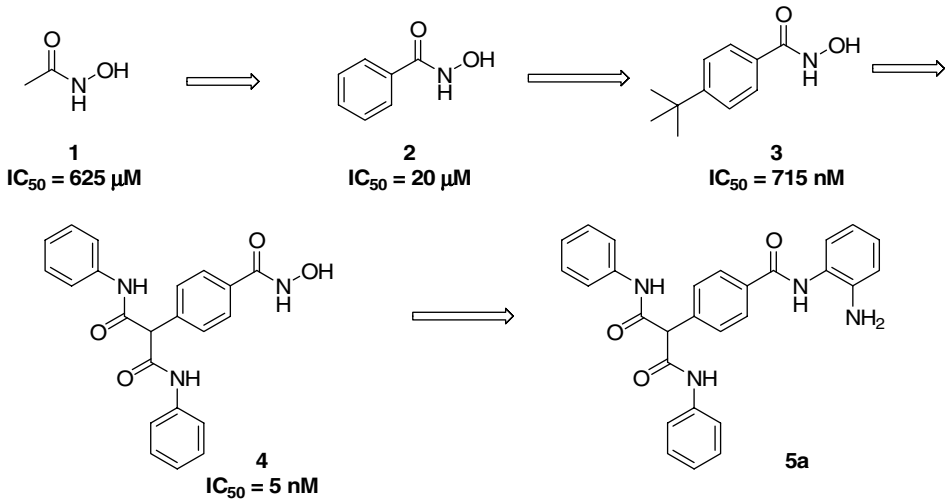

Figure 2. Evolution of HDAC inhibitors.

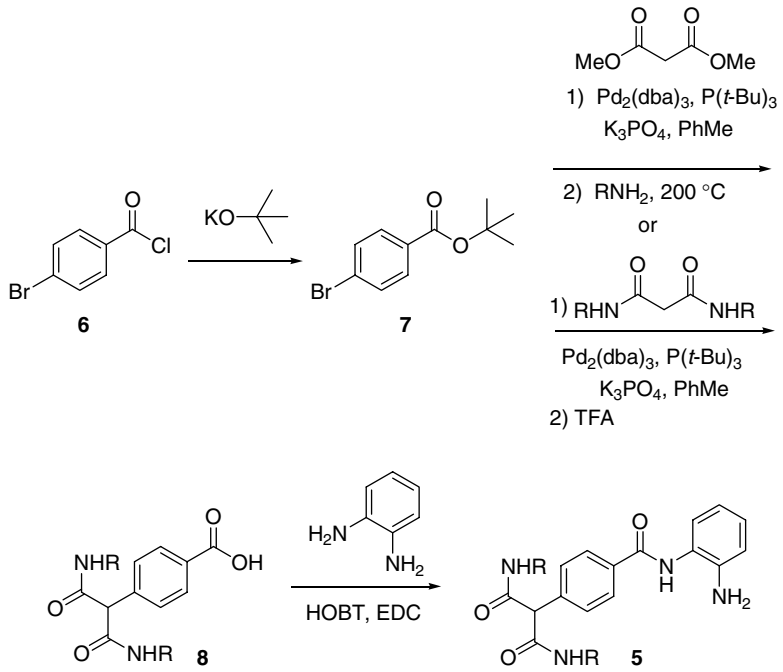

Scheme 1. Synthesis of phenyl benzamide.

tert-butoxide. Palladium mediated coupling[21] between dimethyl malonate and phenyl bromide **7**, followed by thermal displacement of the esters and *tert*-butyl ester cleavage, provided the carboxylic acid **8**. An alternate route to obtain **8** was through palladium mediated coupling with the malonyl diamide followed by *tert*-butyl ester cleavage. Finally, EDC coupling of carboxylic acid **8** with phenylene diamine provided the desired benzamides **5**.

Compound **5a**, the *N*-(2-aminophenyl)amide analogue of **4**, displayed good HDAC inhibitory activity, with an IC_{50} = 41 nM against HDAC1 and an IC_{50} = 171 nM in HCT116-72 h cell proliferation assays.[22]

Encouraged by the activity of benzamide **5a**, our attention was directed toward the synthesis of analogues with diverse substitution around the phenyl ring in the surface recognition domain. Representative analogues (Table 1) demonstrate that a wide array of functionality can be tolerated in the malonyl–phenyl rings including nitrile, methoxy, and morpholine moieties. A reduction in cellular potency can be seen in biaryl **5i**, possibly due to its low hydrophilicity. The *c* log *P*[23] of **5i** is greater than that of the phenyl amide **5a** by two log units. Notably, ortho-substitution of the malonyl–phenyl rings was tolerated in contrast to ortho-substitution of the phenyl ring within vorinostat, which leads to a marked decrease in activity.

Moreover, both amide NH moieties were essential for significant enzymatic and cellular potency (Table 2). Incorporation of a single methyl group on the malonyl sidechains to give **5j** resulted in a 5-fold loss of potency. Similarly, the dimethyl derivative **5k** was 100-fold less potent indicating that hydrogen bonding, either inter- or intra-molecular, may play an important role in the recognition of the HDAC active site. Similarly, it was shown that malonyl di-ester analogues possessed significant reduction in HDAC enzymatic activity as well (data not shown).

In addition the aniline-amide proved to be optimal for HDAC1 activity (Table 3). The one-carbon homologue, benzylamine **5l**, was less active against HDAC1 and this trend continued to **5m**, which was approximately 5-fold less active in the HDAC-enzyme assay and almost 10-fold less active in the cell proliferation assay.

Having explored the SAR in the surface recognition domain, we set out to iteratively re-optimize potency by further exploring the linker domain. Substitution at the benzylic position with a fluoride **5n** or methyl **5p** was assessed in an effort to minimize potential metabolism issues since the methine unit is easily oxidized. Furthermore, a hydroxyl group **5o** was installed with the hope of improving the compound solubility. Additionally, we investigated the effect of inserting a methylene, thus allowing further flexibility of the sidechain (**9a**–**9b**). However, data demonstrated that these derivatives suffer attenuated cell potency (Table 4) and did not offer advantages in subsequent physiochemical and pharmacokinetic analyses (data not shown).

Table 1. Structure–activity relationship of *N*,*N*′ diarylmalonamides

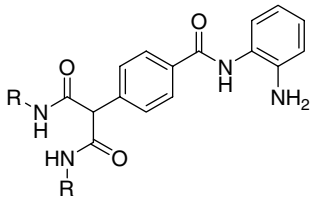

Compound	R	HDAC1 IC_{50} (nM)	HCT116-72 IC_{50} (nM)
5a		41	171
5b	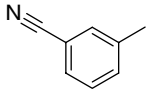	34	500[a]
5c	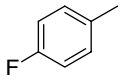	63	222[a]
5d	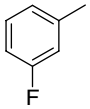	56	607
5e	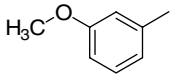	35	383
5f	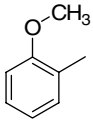	47	394
5g	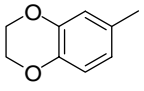	21	220
5h	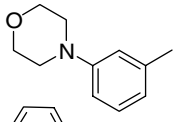	45	542
5i	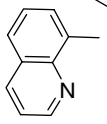	103	1200

[a] HCT116-96 h.

Table 2. SAR of **5a**, **5j**, and **5k**

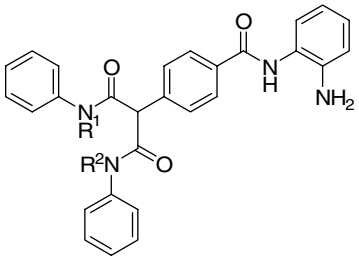

Compound	R^1	R^2	HDAC1 IC_{50} (nM)	HCT116-72 IC_{50} (nM)
5a	H	H	41	171
5j	H	CH_3	196	1145
5k	CH_3	CH_3	7195	NA

Table 3. SAR of malonyl sidechain extension compound

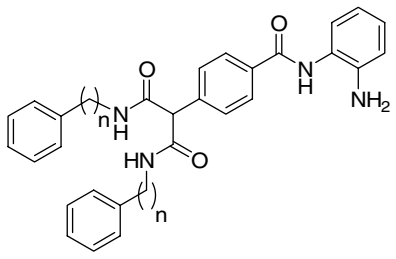

Compound	*n*	HDAC1 IC_{50} (nM)	HCT116-72 IC_{50} (nM)
5a	0	41	115
5l	1	199	596
5m	3	229	987

Table 4. SAR of substituted diarylmalonamide on benzyl analogues

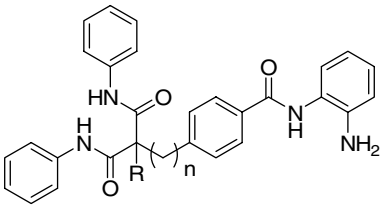

Compound	R	*n*	HDAC1 IC_{50} (nM)	HCT116-72 IC_{50} (nM)
5a	H	0	41	171
5n	F	0	48	425
5o	OH	0	94	773
5p	Me	0	198	2125
9a	H	1	47	579
9b	Me	1	200	2519

The synthesis of α-substituted analogues **5n**–**5p** was achieved through a common intermediate carboxylic acid **7** (Scheme 2). EDC coupling with monoprotected *o*-phenylenediamine provided amide **10**. Deprotonation of the malonate and trapping with an appropriate electrophile followed by TFA deprotection of the Boc moiety furnished the necessary analogues **12**. The hydroxyl substituted compound **5o** was obtained by stirring the carboxylic acid **7** in aqueous LiOH in air followed by EDC coupling with phenylene diamine (Scheme 3).

Synthesis of the benzyl derivatives was achieved through alkylation of the dialkyl malonamide anion with benzyl bromide **13** (Scheme 4). Hydrolysis of the methyl ester followed by EDC coupling furnished the benzamides **9a** and **9b.**

Having established that **5a** exhibited good activity in enzymatic and excellent cellular assays, **5a** was evaluated against other HDAC subtypes.[24] Compound **5a** was found to be inactive against HDAC6 and HDAC8, almost 10-fold selective for HDAC1 over HDAC2, and 20-fold selective over HDAC3 (Table 5). Having a Class I selective compound may offer significant advantages over less selective HDAC inhibitors in terms of tolerability and efficacy since Class I and Class II do have different biological function.

The pharmacokinetic profile of **5a** in several animal species was determined (Table 6). Good oral bioavailability was seen in rat and dog ($F = 88\%$ for both species). In addition, the compound exhibited low plasma clearance in higher order species and an acceptable half-life across species.

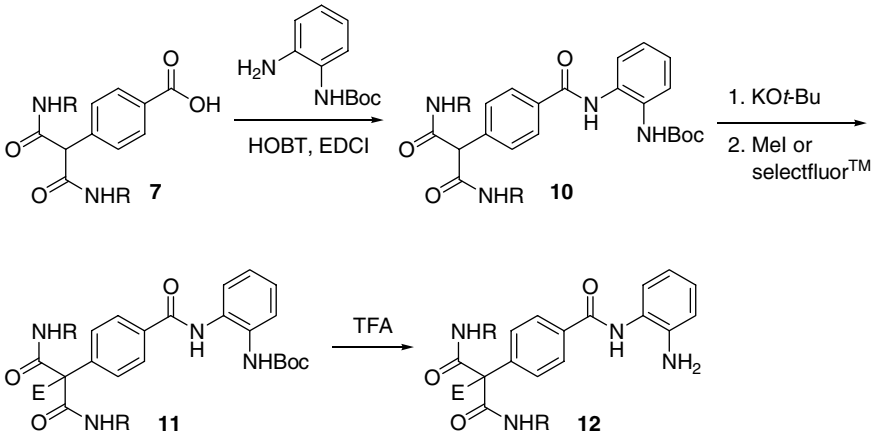

Scheme 2. Incorporation of substitution at the methine position.

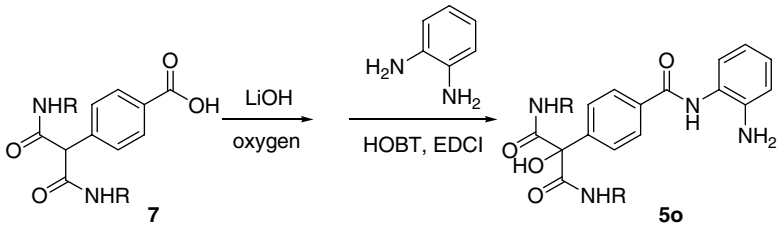

Scheme 3. Synthesis of hydroxyl derivative.

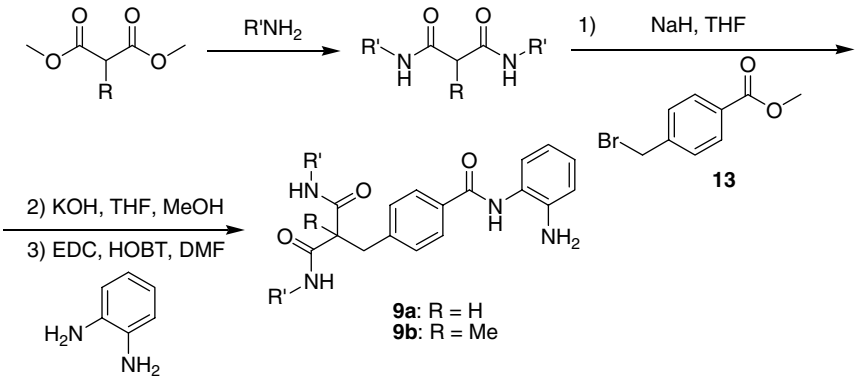

Scheme 4. Synthesis of benzyl derivatives.

Table 5. HDAC selectivity profile for **5a**

HDAC1 IC_{50} (nM)	HDAC2 IC_{50} (nM)	HDAC3 IC_{50} (nM)	HDAC6 IC_{50} (nM)	HDAC8 IC_{50} (nM)
36	313	697	>10,000	>10,000

Table 6. Pharmacokinetic profile for **5a**

	IV dose (mg/kg)	CL (ml/min/kg)	Vd (L/kg)	po dose (mg/kg)	AUC (Norm) (μM h kg/mg)	*F* (%)	*T* 1/2 (h)
Rat	2.0	55	12	4.0	0.48	88	3.8
Dog	0.6	3	1.8	1.2	10.6	88	8.5
Rhesus	1.0	2.5	1.7	2.0	3.88	27	10.4

The evolution of HDAC inhibitor design has largely occurred in the context of the discovery of natural products with HDAC inhibitory activity. In an effort to better understand the HDAC inhibitor pharmacophore beyond historical findings, we have utilized an iterative approach to HDAC inhibitor design. These efforts have yielded novel, potent HDAC inhibitor structures that extend the current HDAC inhibitor pharmacophore to include agents with sterically bulky branched functionalities at the linker/surface recognition domain interface. Further profiling of **5a** will be reported in due course along with other novel HDAC inhibitors.

References and notes

1. Grant, S.; Easley, C.; Kirkpatrick, P. *Nat. Rev. Drug Disc.* **2007**, *6*, 21.
2. Huang, L. *J. Cell. Physiol.* **2006**, *209*, 611.
3. Liu, T.; Kuljaca, S.; Tee, A.; Marshall, G. M. *Cancer Treat. Rev.* **2006**, *32*, 157.
4. Bolden, J. E.; Peart, M. J.; Johnstone, R. W. *Nat. Rev. Drug Disc.* **2006**, *5*, 769.
5. Minucci, S.; Pelicci, P. G. *Nat. Rev. Cancer* **2006**, *6*, 38.
6. Miller, T. A.; Witter, D. J.; Belvedere, S. *J. Med. Chem.* **2003**, *46*, 5097.
7. Richon, V. M.; Webb, Y.; Merger, R.; Sheppard, T.; Jursic, B.; Ngo, L.; Civoli, F.; Breslow, R.; Rifkind, R. A.; Marks, P. A. *Proc. Natl. Acad. Sci. U.S.A.* **1996**, *93*, 5705.
8. Vannini, A.; Volpari, C.; Filocamo, G.; Casavola, E. C.; Brunetti, M.; Renzoni, D.; Chakravarty, P.; Paolini, C.; De Francesco, R.; Gallinari, P.; Steinkuhler, C.; Di Marco, S. *Proc. Natl. Acad. Sci. U.S.A.* **2004**, *101*, 15064.
9. Yoshida, M.; Horinouchi, S.; Beppu, T. *Bioessays* **1995**, *17*, 423.
10. Grozinger, C. M.; Schreiber, S. L. *Chem. Biol.* **2002**, *9*, 3.
11. Kijima, M.; Yoshida, M.; Sugita, K.; Horinouchi, S.; Beppu, T. *J. Biol. Chem.* **1993**, *268*, 22429.
12. Yoshida, M.; Kijima, M.; Akita, M.; Beppu, T. *J. Biol. Chem.* **1990**, *265*, 17174.
13. Nakajima, H.; Kim, Y. B.; Terano, H.; Yoshida, M.; Horinouchi, S. *Exp. Cell Res.* **1998**, *241*, 126.
14. Darkin-Rattray, S. J.; Gurnett, A. M.; Myers, R. W.; Dulski, P. M.; Crumley, T. M.; Allocco, J. J.; Cannova, C.; Meinke, P. T.; Colletti, S. L.; Bednarek, M. A.; Singh, S. B.; Goetz, M. A.; Dombrowski, A. W.; Polishook, J. D.; Schmatz, D. M. *Proc. Natl. Acad. Sci. U.S.A.* **1996**, *96*, 13143.
15. Yoshida, M.; Nomura, S.; Beppu, T. *Cancer Res.* **1987**, *47*, 3688.
16. Hann, M. M.; Leach, A. R.; Harper, G. J. J. *Chem. Inf. Comput. Sci.* **2001**, *41*, 856.
17. Finnin, M. S.; Donigian, J. R.; Cohen, A.; Richon, V. M.; Rifkind, R. A.; Marks, P. A.; Breslow, R.; Pavletich, N. P. *Nature* **1999**, *401*, 188.
18. (a) Saito, A.; Yamashita, T.; Mariko, Y.; Nosaka, Y.; Tsuchiya, K.; Ando, T.; Suzuki, T.; Tsuruo, T.; Nakanishi, O. *Proc. Natl. Acad. Sci. U.S.A.* **1999**, *96*, 4592; (b) Suzuki, T.; Mariko, Y.; Tsuchiya, K.; Fukazawa, N. *J. Med. Chem.* **1999**, *42*, 3001; (c) Acharya, M.; Sparreboom, A.; Sausville, E. A.; Conley, B. A.; Doroshow, J. H.; Venitz, J.; Figg, W. D. *Cancer Chemother. Pharmacol.* **2006**, *57*, 275.
19. Moradei, O.; Leit, S.; Zhou, N.; Frechette, S.; Paquin, I.; Raeppel, S.; Gaudette, F.; Bouchain, G.; Woo, S. H.; Vaisburg, A.; Fournel, M.; Kalita, A.; Lu, A.; Trachy-Bourget, M.-C.; Yan, P. T.; Liu, J.; Li, Z.; Rahil, J.; MacLeod, A. R.; Besterman, J. M.; Delorme, D. *Bioorg. Med. Chem. Lett.* **2006**, *16*, 4048.

20. For other studies with malonyl diamide see (a) Wang, D.-F.; Wiest, O.; Helquist, P.; Lan-Hargest, H. Y.; Wiesch, N. L. *J. Med. Chem.* **2004**, *47*, 3409; (b) Wang, D.-F.; Helquist, P.; Wiech, N. L.; Wiest, O. *J. Med. Chem.* **2005**, *48*, 6936.
21. Beare, N. A.; Hartwig, J. F. *J. Org. Chem.* **2002**, *67*, 541.
22. HDAC cell-based proliferation results were determined by the following procedure: HCT116 cells were plated in 96-well plates at density of 1000 cells/well. The next day, cells were treated with either 0.2% DMSO or increasing concentrations of **7i** dissolved in DMSO (final concentration of DMSO 0.2%). After 72 h incubation at 37 °C with 5% CO_2, viable cells were quantitated using Vialight Plus (Cambrex) according to manufacturer's instructions.
23. *c*log *P* was calculated using ACD lab software.
24. HDAC enzymatic activities were determined by the following procedure: 3× serial dilutions of a 10 mM solution of inhibitor were performed in DMSO followed by a 20× dilution into assay buffer. Twenty microliters of HDAC was preincubated with 5 μl diluted compound at RT for 10 min. The reaction was initiated by the addition of 25 μl of the appropriate substrate (HDACs 1, 2, 3, and 6: Fluor-de-Lys substrate KI-104; HDAC8: Fluor-de-Lys HDAC8 substrate KI-178), incubated 15 (HDAC8) or 60 (HDACs 1, 2, 3, and 6) minutes at 37 °C, before adding 50 μl of the appropriate development solution. The development solution for HDACs 1, 2, 3, and 6 was 167×-diluted 20× Developer Concentrate (BIOMOL: KI-105) plus 10 μM SAHA. For HDAC8, the development solution was 100×-diluted 5× Developer Concentrate (BIOMOL: KI-176) plus 10 μM SAHA. The assay was read in a VictorV plate reader (Perkin-Elmer, Wellesley, MA) at Ex 360 nm/Em 460 nm.
The substrate for HDAC1, HDAC2, HDAC3, and HDAC6 was 30 μM Fluor-de-Lys substrate (BIOMOL: KI-104) and for HDAC8, 30 μM Fluor-de-Lys HDAC8 substrate (BIOMOL: KI-178). The development solution for HDAC1, HDAC2, HDAC3, and HDAC6 was 167×-diluted 20× Developer Concentrate (BIOMOL: KI-105) plus 10 μM SAHA. For HDAC8, the development solution was 100×-diluted 5× Developer Concentrate (BIOMOL: KI-176) plus 10 μM SAHA. HDAC final concentration in the reaction was 1–30 nM. HDAC8 was a generous gift of Paola Gallinari from Institute for Research in Molecular Biology, Pomezia, Italy. Carboxy-terminal FLAG-tagged human HDACs 1, 2, 3 (co-expressed with the domain of SMRT), and 6 were overexpressed in mammalian cells and affinity-purified using an anti-Flag antibody matrix, eluted from the matrix with 100 μg/ml of a competing FLAG peptide in 20 mM Tris–Cl, pH 8.0, 150 mM NaCl, 10% glycerol, and protease inhibitor cocktail (Roche cat. No. 1836153).